Supplementary Materials for

Laser patterning bioprinting using a light sheet-based system equipped with a light sheet imaging system produces long-term viable skin constructs

Levin Hafa *et al.*

*Corresponding author: Francesco Pampaloni, fpampalo@bio.uni-frankfurt.de

This PDF file includes:

Supplementary Text
Figs. S1 to S11
Tables S1 to S8
Legends for Movies S1 to S3

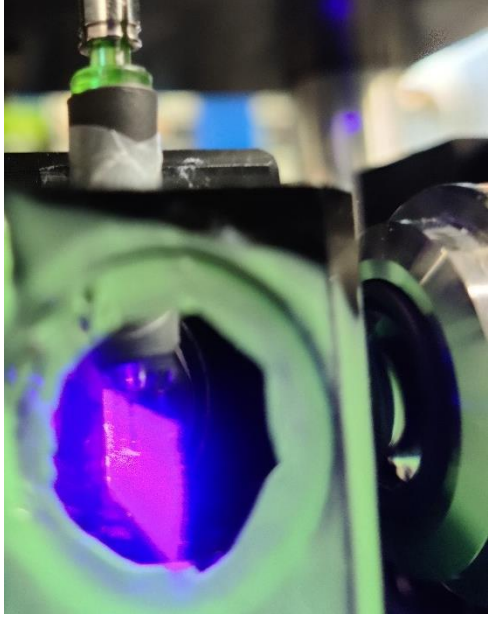**Other Supplementary Materials for this manuscript include the following:**

Movies S1 to S3

Fig. S1. Picture of the static light sheet (view from the side), crossing the specimen chamber.
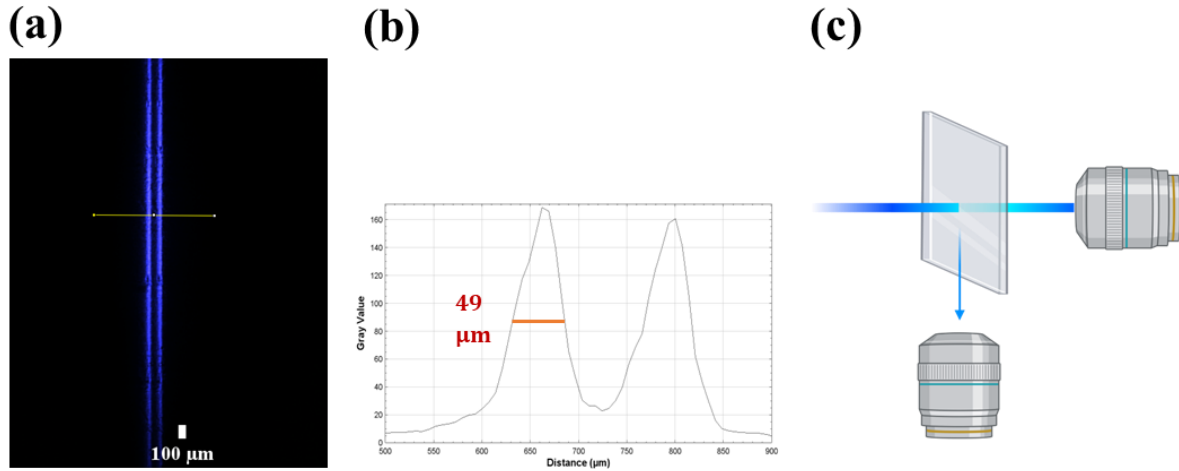
(a)

(b)

(c)

Fig. S2. Measurements of the static light sheet. (**a**) Light sheet microscope image showing the width for the static light sheet at 405 nm wavelength. (**b**) Full width half maximum (FWHM) measurement to define exact width of the light sheet. Measurement in the middle of the light sheet was found to be 49 µm. (**c**) The impression of a double light sheet is due to refraction from a cover glass.
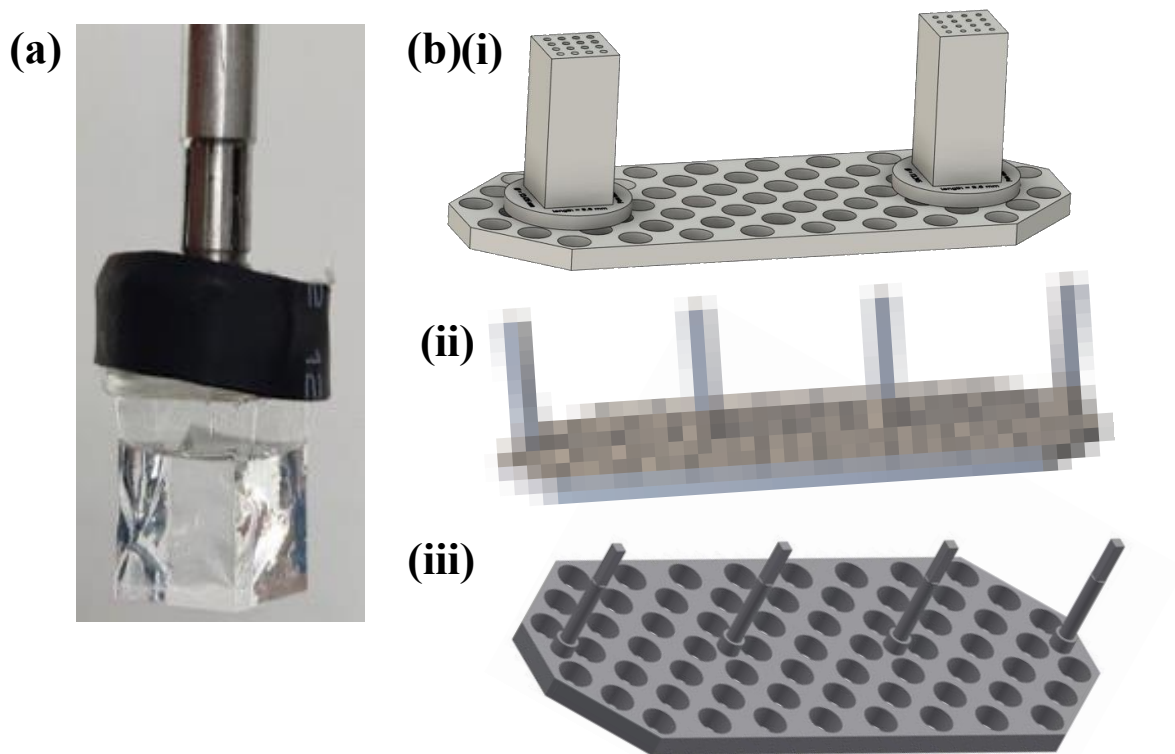
Fig. S3. The cuvette used as a sample holder for 3D bioprinting with the light sheet device.
(**a**) Picture of the 10x10x10 mm model of the cuvette, filled with water. The FEP foil cuvette is connected to the sample holder metal rod through the addition of a shrinking tube (in black). (**b**) The cuvettes are produced using the thermo-forming method described by Hötte et al. (*28*). (**i**) Positive mold for the 10x10x10 mm cuvette. The holes are used to maximize the efficiency of the vacuum during thermoforming. (**ii**) 3x3x5 mm cuvette mold. (**iii**) 1,5x1,5x5 mm cuvette mold.
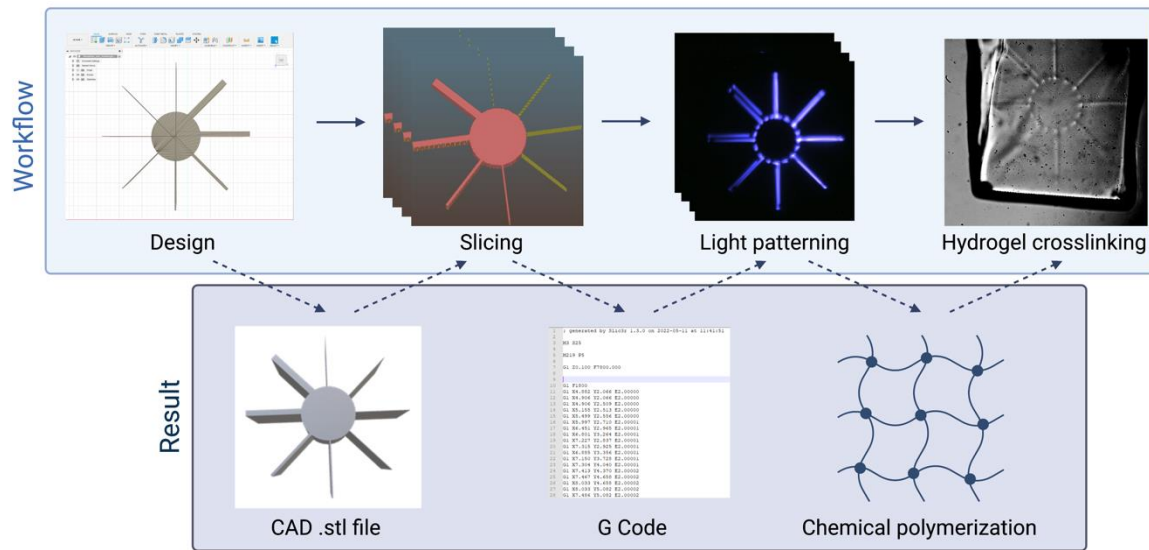
Fig. S4. The workflow for bioprinting. It involves four steps from design to crosslinking: designing the 3D object (obtaining a CAD file), slicing the object into z planes (obtaining a G-code), translating into light beam patterning and therefore crosslinking which produces a 3D bioprint. Figure created with Biorender.
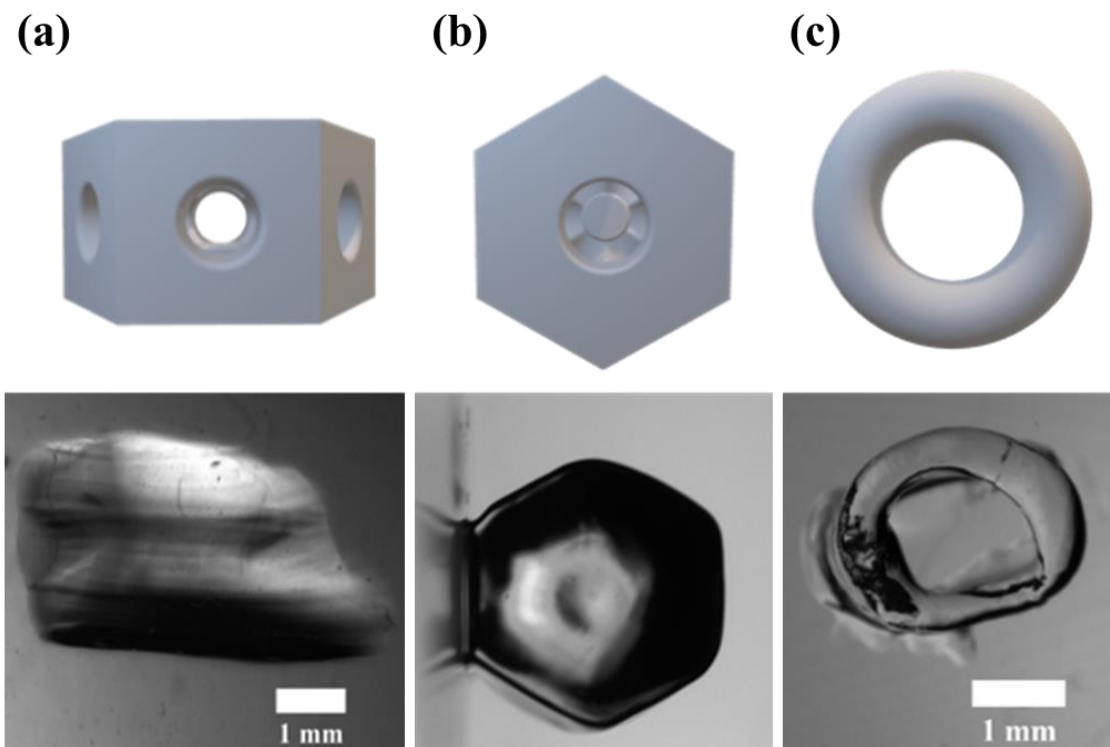
Fig. S5. Brightfield pictures of the bioprinted constructs. Constructs were printed using GELMA/PEGDA hydrogel and imaged in air outside of the cuvette. (**a**) Side view and (**b**) top view of the liver lobule. (**c**) Top view of the torus. The resolution wheel did not withstand the extraction process and could not be imaged; however, the liver lobule and torus maintained their shape. Microscope: Zeiss SteREO Discovery V8. Objective: Plan Apo S, 0.63×/0.116 FWD 81 mm. Camera: AxioCam IcC SIN.
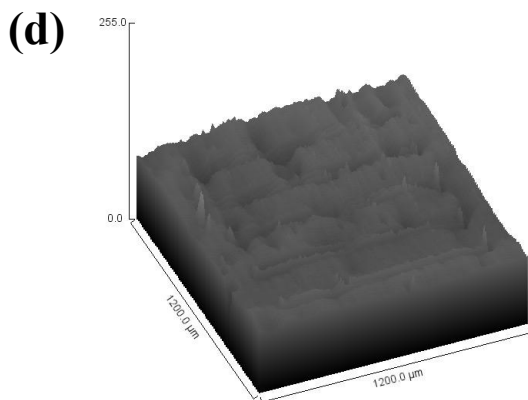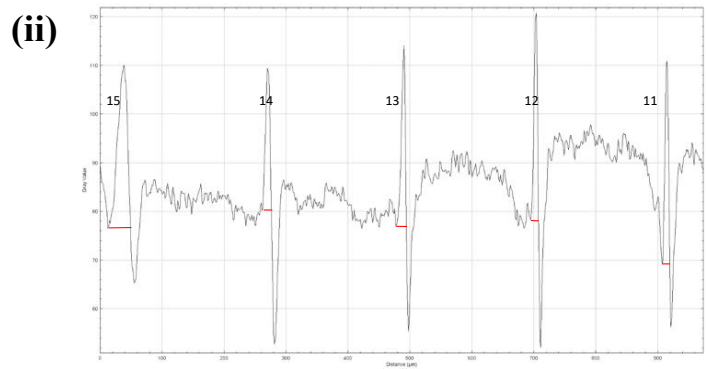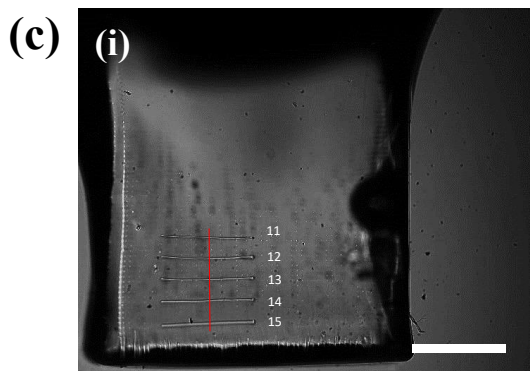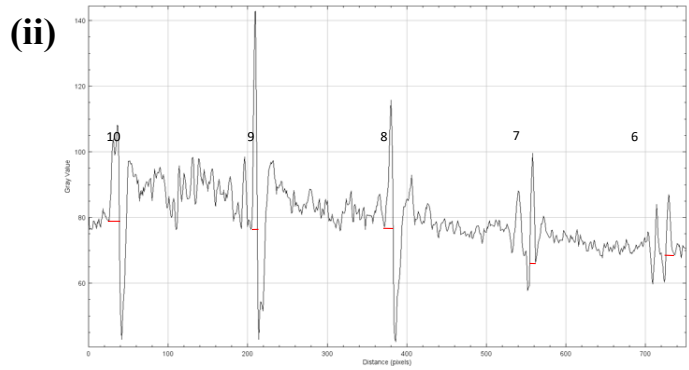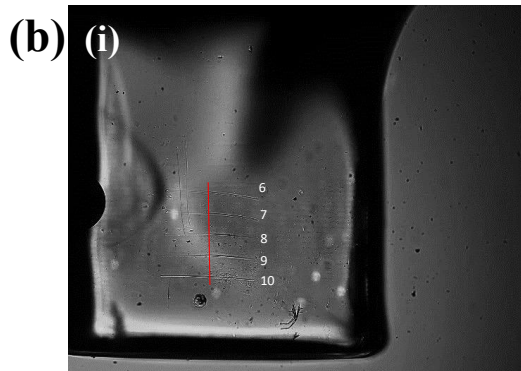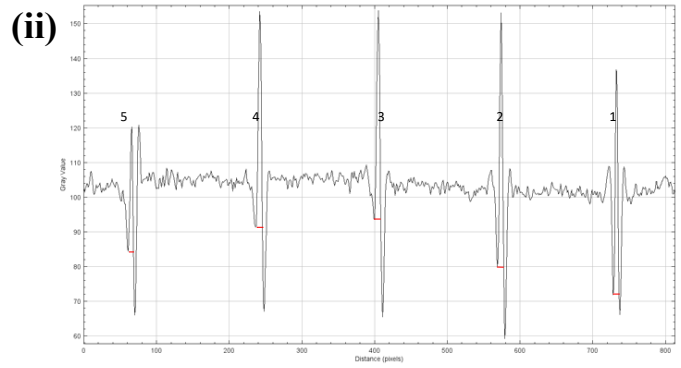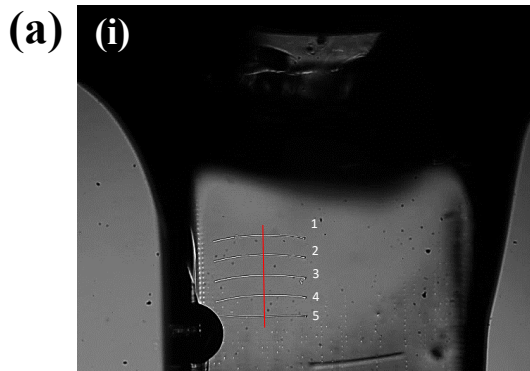
Fig. S6. Printing resolution of the patterned light-beam with resin. (**a**), (**b**) and (**c**) represent five lines printed as triplicates, with (**a**) – (**c**)(**i**) being the brightfield image of the printed lines and (**a**) – (**c**)(**ii**) the analysis of the width of each line. Red lines in (**a**) – (**c**)(**i**) show where the measurement for the width was conducted, red lines in (**a**)(**ii**) – (**c**)(**ii**) show the measured widths for each line in ImageJ and numbers referring to the lines from brightfield images in (**a**)(**i**) – (**c**)(**i**). (**d**) Example surface plot for (**a**)(**i**). (**e**) Calculations for mean, median and standard deviation for the width of the 15 lines printed. Brightfield images captured in the bioprinter. Scale bar: 1 mm.
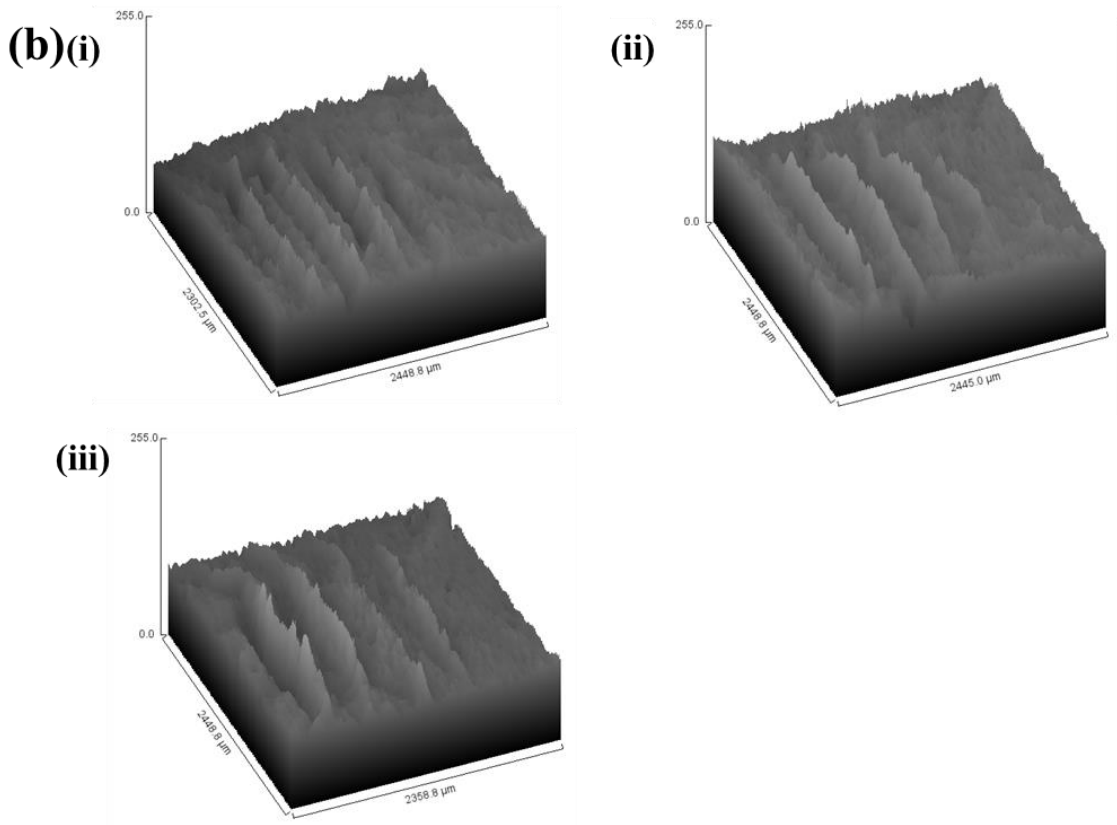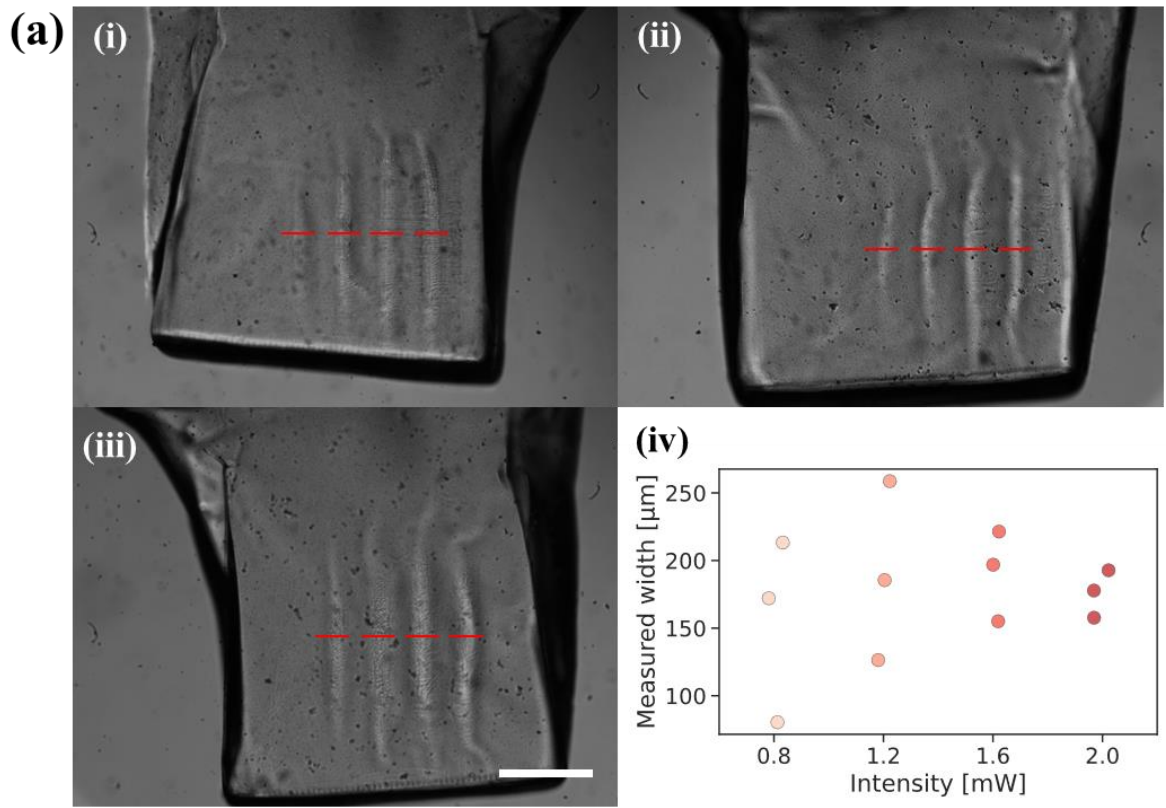
Fig. S7. Measurements of the crosslinked orthogonal static light sheet. It was printed using Cellendes hydrogel 1 with 0.8, 1.2, 1.6 and 2 mW, respectively. (**a**)(**i**), (**ii**) and (**iii**) Three replicates à five laser power settings (2, 1.6, 1.2, 0.8, 0.4 mW) were conducted, respectively. For 0.4 mW no crosslinked sheet was observed. Red lines indicate the position of measurement. (**a**) (**iv**) The total average for the sheet width was measured to be 178.2 µm ± 46.2 µm, with the smallest sheet at 80.8 µm width using 0.8 mW of laser power. (**b**)(**i**), (**ii**) and (**iii**) Surface plots for (**a**)(**i**) to (**iii**). Brightfield images captured in the bioprinter. Scale bar: 1 mm.
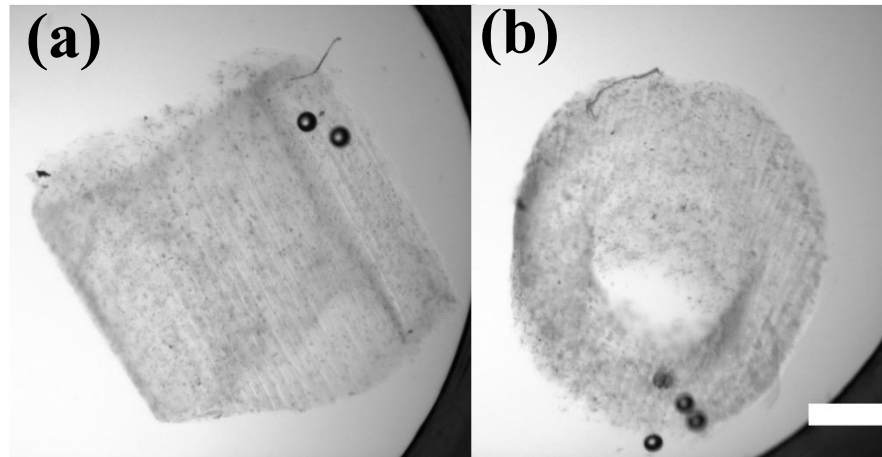
Fig. S8. Stereomicroscope images of the bioprinted cylinder. (**a**) Side view of the construct. The bottom of the object was truncated during manipulation. (**b**) Top view of the construct. The hollow part of the cylinder is well resolved and the object is not collapsing. Microscope: Zeiss SteREO Discovery V8. Objective: Plan Apo S, 0.63×/0.116 FWD 81 mm. Camera: AxioCam IcC SIN. Scale bar: 500 µm.

| Dead | Live | Nuclei | Live/Dead/All |
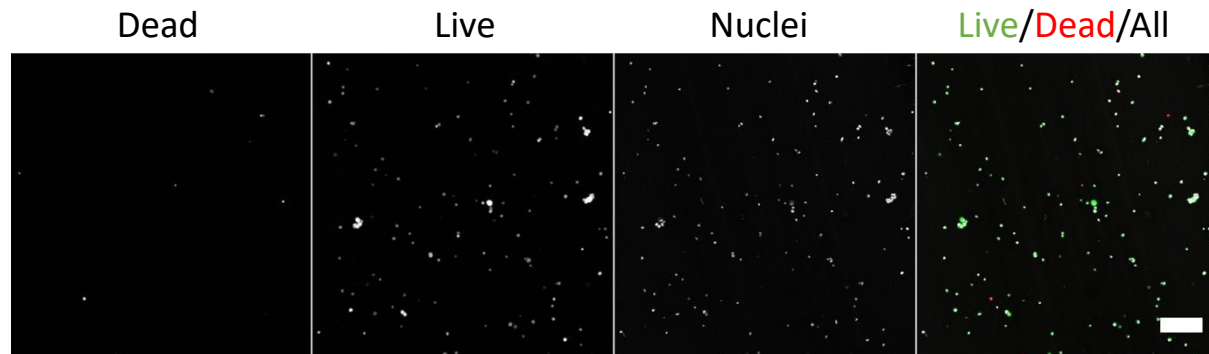
Fig. S9. Image of the live dead assay of Hs27 fibroblasts encapsulated in Cellendes hydrogel 2 right after bioprinting (day 0). The dead cells are stained with propidium iodide (PI), the live cells with fluorescein diacetate (FDA) and the nuclei with Hoechst 33342. Microscope: Zeiss AxioObserver LSM780. Objective: Plan ApoChromat 20×/0.8 M27. Voxel size "Hs27 Single Beam": $0.52 \times 0.52 \times 6$ µm. Voxel size "Hs27 Beam & static LS" and "Co-culture Hs27 & HaCaT": $0.83 \times 0.83 \times 6$ µm. Scale bar: 100 µm.
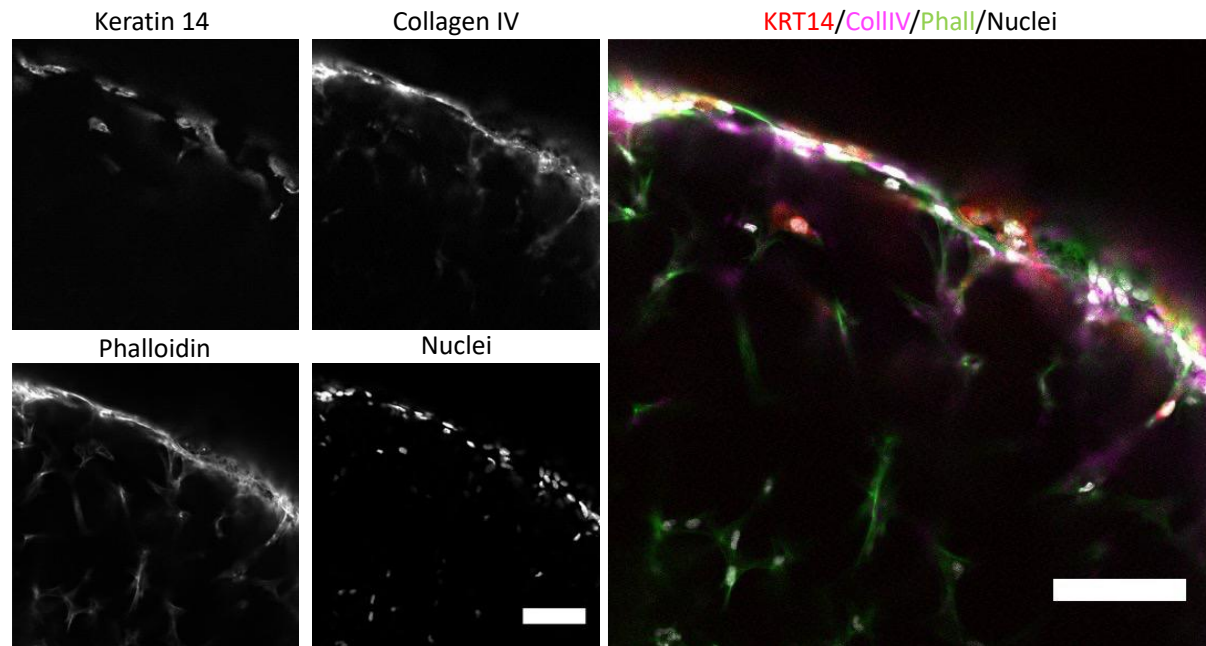
Fig. S10. Cross section of the cylinder with immunofluorescently stained fibroblasts (Hs27) and keratinocytes (HaCaT). Keratin 14 (KRT14), Collagen IV (CollIV), phalloidin (Phall) and the nuclei (Hoechst 33342) were stained. A layer of keratinocytes, identifiable by the presence of Keratin 14, is forming on the outside of the object. Microscope: Zeiss AxioObserver LSM780. Objective: Plan ApoChromat 20×/0.8 M27. Scale bar: 100 µm.

Theoretical principle of Light sheet bioprinting

The photopolymerization process is limited by the photon density in the print volume. A theoretical photon density threshold can be specified by determining the light sheet properties. Multiple definitions of the beam waist radius ω_0 exist (FWHM, 1/e2, D4σ). The 1/e2 width is a reasonable approximation:

$$\omega_0 \cong (1 - e^{-2}) \times \frac{\lambda_{exc}}{2 \times NA_{ill}}$$

Using the objective lens properties from the setup ($NA_{ill} = 0.06$) and the excitation wavelength of the laser beam $\lambda_{exc} = 395$ nm, a theoretical beam waist radius ω_0 of 2846 nm and a beam waist diameter $\varnothing_{beam}$ of 5692 nm was calculated. The Rayleigh length x_R is defined as the distance along the propagation of a gaussian beam from its waist to the spot where the area of its cross section is doubled:

$$x_R = \frac{n \times \pi \times \omega_0^2}{\lambda_{exc}}$$

Inserting the refractive index for water ($n = 1.33$), the beam waist radius ω_0 (2846 nm) and the excitation wavelength of the laser beam $\lambda_{exc} = 395$ nm a Rayleigh length of 85690 nm or 85.69 µm was calculated. One light sheet x_{FOV} can be approximated by multiplying the Rayleigh length by two, resulting in 171 µm.
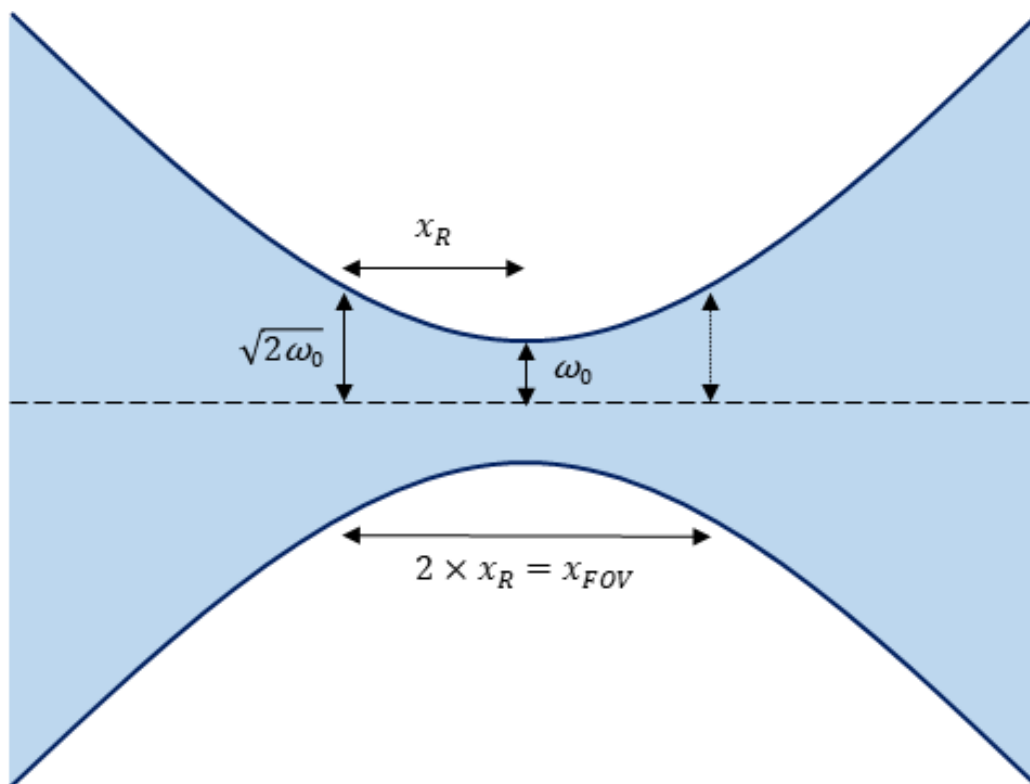
Fig. S11. Gaussian beam profile. Beyond the Rayleigh length, the beam cross-section increases almost fourfold with increasing distance from the focal plane. Thus, the number of photons per unit area also decreases in the same order, resulting in a non-linear reduction of radicals and at the same time in a non-linear photo crosslinking process (*69,70*).

Table S1. Laser power measurements for the single laser beam.

S-Value	Power in %	Measured power [mW]	Measured power - Blank [mW]	Designed Power [mW]	Difference: Designed - Measured power [mW]	Percentage of power left at print focal spot
255	100	23.27	23.27	60	36.7	38.78
242	95	22.16	22.16	57	34.8	38.87
230	90	20.91	20.91	54	33.1	38.72
217	85	19.95	19.95	51	31.1	39.11
204	80	18.6	18.60	48	29.4	38.75
191	75	17.62	17.62	45	27.4	39.15
179	70	16.33	16.33	42	25.7	38.88
166	65	15.2	15.20	39	23.8	38.97
153	60	14.13	14.13	36	21.9	39.25
140	55	12.9	12.90	33	20.1	39.09
128	50	11.85	11.85	30	18.2	39.50
115	45	10.56	10.56	27	16.4	39.11
102	40	9.49	9.49	24	14.5	39.54
89	35	8.23	8.23	21	12.8	39.18
77	30	7.18	7.18	18	10.8	39.88
64	25	5.89	5.89	15	9.1	39.26
51	20	4.81	4.81	12	7.2	40.07
38	15	3.62	3.62	9	5.4	40.21
25	10	2.47	2.47	6	3.5	41.14
13	5	1.27	1.27	3	1.7	42.28
0	0	0.0015	0	0	0.0	-

Table S2. Laser power measurements for the static light sheet beam.

S-Value	Power in %	Measured power [mW]	Measured power - Blank [mW]	Designed Power [mW]	Difference: Designed - Measured power [mW]	Percentage of power left at print focal spot
51.0	20	4.240	4.239	10	5.8	42.39
38.3	15	3.180	3.179	7.5	4.3	42.38
25.5	10	2.110	2.109	5	2.9	42.17
12.8	5	1.045	1.044	2.5	1.5	41.74
2.6	1	0.181	0.180	0.5	0.3	35.90
2.3	0.9	0.162	0.161	0.45	0.3	35.67
2.0	0.8	0.141	0.140	0.4	0.3	34.88
1.8	0.7	0.117	0.116	0.35	0.2	33.00
1.5	0.6	0.101	0.100	0.3	0.2	33.17
1.3	0.5	0.083	0.082	0.25	0.2	32.60
1.0	0.4	0.062	0.061	0.2	0.1	30.25
0.8	0.3	0.046	0.045	0.15	0.1	29.67
0.5	0.2	0.032	0.031	0.1	0.1	30.50
0.3	0.1	0.020	0.019	0.05	0.0	37.00

Table S3. Energy calculations for every 3D print in this publication.

Printed object	S-Value	Power in %	Measured power [mW]	Energy [mJ/cm^2]	Exposure time [s]
Wheel of resolution (Hydrogel)	45	17.6	4.22	5.02	-
Liver lobule (Hydrogel)	51	20	4.81	5.72	-
Torus (Hydrogel)	60	23.5	5.59	6.65	-
Hollow cylinder (Hydrogel resolution)	45	17.6	4.22	5.02	-
(hydrogel with cells – medium	51	20	4.65	5.72	-
pellet – big pellet)	92	36	8.37	10.30	-
Five lines (Resin)	45	17.6	4.22	5.02	-
Static LS (Resin)	-	0.1	0.02	0.017; 0.013; 0.010; 0.007; 0.004	5; 4; 3; 2; 1
Static LS (Hydrogel)	51; 41; 31; 20; 10	20; 16; 12; 8; 4	4.24; 3.39; 2.53; 1.68; 0.83	7.35; 6.88; 4.38; 2.91; 1.44	10

Table S4. List of antibodies and dyes

Component	Supplier	Stock	Dilution
MitoTracker red FM	Invitrogen	1 mM	1:1000
Fluorescein diacetate	Sigma-Aldrich Chemie GmbH	5mg/ml in acetone	1:500
Propidium iodide	Sigma-Aldrich Chemie GmbH	1 mg/ml in PBS	1:100
Hoechst 33342	ThermoFisher Scientific	-	1:500
Alexa Fluor 546 Phalloidin	ThermoFisher Scientific	-	1:200
Alexa Fluor 647 Phalloidin	ThermoFisher Scientific	-	1:100
Collagen IV (rabbit)	Abcam	1 mg/ml	1:400
Cytokeratin 14 (mouse)	Santa Cruz Technologies	200 µg/ml	1:50
Vimentin (rabbit)	Cell Signaling	-	1:100
Anti-rabbit Alexa Fluor 488 (goat)	ThermoFisher Scientific	2 mg/ml	1:400
Anti-mouse Alexa Fluor 568 (donkey)	ThermoFisher Scientific	2 mg/ml	1:400

Table S5. Composition of the hydrogel used for resolution experiment (Cellendes hydrogel 1)

Gel components	Final concentration
RGD-N-Dex	3.5 mM (reactive group)
CD-HyLink	5 mM (reactive group)
LAP	0.5 mM
Agarose	0%

Table S6. Composition of the hydrogel used for resolution experiment (GelMA/PEGDA)

Gel components	Final concentration
GelMA	10%(w/v)
PEGDA	10%(w/v)
LAP	0.2%(w/v)
Tartrazine	0.0125%(w/v)

Table S7. Composition of the hydrogel used for hydrogel testing and cell encapsulation (Cellendes hydrogel 2)

Gel components	Final concentration
RGD-N-Dex	3.5 mM (reactive group)
CD-HyLink	3.5 mM (reactive group)
LAP	0.5 mM
Agarose	0.1%

Table S8. Comparison of the BRIGHTER light sheet bioprinter with other state of the art 3D (bio-)printers.

3D (Bio)printer	Technique	Speed [mm³/s]	Print time increase with volume	Resolution [µm]	Energy Dose [mJ/cm²]	Cell viability [%]	Print time for 100 mm³ with best resolution [s]	Print time for 100 mm³ with best resolution [min]	Reference
LS-Bioprinter	orthogonal laser-patterning	0.66	Linear	15.7	5 - 10	>90	152	2.53	This work
Extrusion	Fused deposition modelling	10 - 20	Linear	>100	-	>70	7	0.11	Gómez-Blanco et al. 2021
Stereolithographic (SLA)	LCD photomask	0.21	Linear in height	100 - 200	50	>95	476	7.9	Breideband et al. 2022
Stereolithographic (SLA)	Digital Light processing (DLP)	0.018	Linear in height	25	10 - 100	>85	5556	92.6	Torras et al. 2022
Two Photon	Two Photon-Photopolymerization	0.000045 - 0.125	Linear	0.8 - 10	NA	>70	4444444	74074	Dobos et al. 2020
Volumetric Bioprinting	Tomographic additive manufacturing	6 - 182	Same time up to 3.9 cm³ (14 x 14 x 20 mm)	40 - 100	100 - 500	>90	22.7	0.38	Loterie et al. 2020, Bernal et al. 2022, Gehlen et al. 2023
Volumetric Bioprinting	Xolography	55	Same time up to 1 cm³	20	50 - 300	Not suitable for bioprinting	2	0.03	Regehly et al. 2020

Movie S1. Video of the patterning of a resolution wheel, as seen from the integrated camera (view from the side, patterning not at full speed).

Movie S2. Static light sheet and laser patterning beam (view from the top, patterning not at full speed).

Movie S3. Z-stack of the Hs27-mitotracker and HUVEC-GFP co-culture imaged in the light sheet part of the bioprinter (color-coded by depth). Only the 488 nm channel showing the HUVEC-GFP cells is here shown. Voxel size: 0.69 × 0.69 × 10 μm. Objective lenses: Zeiss A-Plan 2.5x/0.06 (excitation).